CO_2 Dynamics

DOI: 10.1002/anie.201300446

Understanding CO_2 Dynamics in Metal–Organic Frameworks with Open Metal Sites**

Li-Chiang Lin, Jihan Kim, Xueqian Kong, Eric Scott, Thomas M. McDonald, Jeffrey R. Long, Jeffrey A. Reimer, and Berend Smit*

The selective adsorption of CO_2 is one of the proposed methods for carbon capture that should result in the mitigation of greenhouse gases in the atmosphere. Developments in the field suggest that porous materials such as zeolites and metal–organic frameworks (MOFs) are promising materials for carbon capture due to their large capacity to selectively adsorb CO_2.[1] In particular, MOFs[2] with open metal sites such as Mg_2(dobdc) (dobdc^{4-} = 2,5-dioxido-1,4-benzenedicarboxylate; Mg-MOF-74) possess strong CO_2-binding sites leading to large experimental CO_2 uptake values. Recently, a number of research papers devoted specifically to this structure and its variants have been reported.[3] Most of the past research on open-metal-site structures, however, has focused on the equilibrium properties of the CO_2 adsorption rather than its dynamics. The dynamics of CO_2 molecules within these structures is an important topic that can lead to better designs for open-metal-site MOFs, while exposing possible diffusion limitations.

A recent study presented ^{13}C NMR spectra and relaxation times for CO_2 adsorbed inside Mg-MOF-74.[4] The observed CO_2 chemical shift anisotropy (CSA) patterns "flipped" at temperatures above 150 K, yielding CSA patterns consistent with simple uniaxial rotation of the O=C=O molecule about a fixed rotational angle. At a CO_2 loading of 0.3 CO_2/Mg site, a second motion-averaged powder pattern was observed at temperatures above 350 K. The uniaxial rotational model, when applied to the "flipped" CSA patterns, yielded a rotational angle that varied from 59° (0.5 CO_2/Mg site, 300 K) to 69° (0.3 CO_2/Mg site, 210 K). Carbon-13 spin-lattice relaxation times for Mg-MOF-74 with a loading of 0.5 CO_2/Mg site in the temperature range of 12 K–200 K were fit to a Bloembergen–Purcell–Pound (BPP)-type relaxation mechanism governed by two different exponentially activated motions. The authors did not provide any details as to why such processes would be occurring within the Mg-MOF-74 framework. In a further study, visual inspection of molecular dynamics trajectories was made to conclude that the high binding strength between CO_2 and open metal sites, as well as the presence of the rotational motion, reduce the transversal mobility of CO_2 along the channels and thereby reduce diffusivity.[5]

From a structural and thermodynamic point of view, the presence of uniaxial rotation of CO_2 in Mg-MOF-74 is not intuitive. Both density functional theory (DFT)[6] and neutron powder diffraction data at 20 K[7] indicate that the angle θ, shown in Figure 1a, between the minimum-energy CO_2 configuration and the Mg–O(CO_2) vector is in a range of 50–60°, consistent with the angle extracted from the experimental CSA pattern fit to uniaxial rotation. It seems clear, though, that the chemical environment near a metal site is not perfectly symmetric with respect to the Mg–O(CO_2) vector, implying that the CO_2 is unlikely to possess a uniform free energy surface (that is, the "cone" for uniaxial rotation is not of constant free energy). More vexing is the fact that fitting the CSA patterns to a simple uniaxial rotation yields a decreasing CO_2 rotational angle with increasing temperature.[4] At higher temperatures, one would expect CO_2 to explore a larger portion of phase space, which would correspond to an increase in the rotational angle. However, the experiments were interpreted as a decrease in the angle, suggesting a counterintuitive reduction in entropy.

In light of these observations, we utilized molecular simulations to arrive at a different explanation for the experimental results. Canonical Monte Carlo simulations[8] were carried out at various loadings (infinite dilution, 0.3 CO_2/Mg site, and 0.5 CO_2/Mg site) to probe the free energy landscape of CO_2 molecules in Mg-MOF-74 at temperatures ranging from 100 K to 375 K.[9] In these simulations, both dispersive and electrostatic energies were included to model the guest–framework and the guest–guest interactions. Similar to previous studies, we assumed the framework to be rigid and used the DFT optimized structure for our calculations.[10] The Lennard-Jones potential was adopted to describe the dispersion interaction, in which we used the universal force field (UFF)[11] for the framework atoms and the TraPPE model[12] for the CO_2 molecule. The

[*] L.-C. Lin, Dr. X. Kong, E. Scott, Prof. Dr. J. A. Reimer, Prof. Dr. B. Smit
Department of Chemical and Biomolecular Engineering
University of California, Berkeley
Berkeley, CA 94720 (USA)
E-mail: lichianglin@berkeley.edu
Dr. J. Kim, T. M. McDonald, Prof. Dr. J. R. Long, Prof. Dr. B. Smit
Materials Sciences Division, Lawrence Berkeley National Laboratory (USA)
Dr. X. Kong, Prof. Dr. J. A. Reimer
Environmental Energy Technologies Division, Lawrence Berkeley National Laboratory (USA)
T. M. McDonald, Prof. Dr. J. R. Long, Prof. Dr. B. Smit
Department of Chemistry, University of California, Berkeley (USA)

[**] This research was supported through the Center for Gas Separations Relevant to Clean Energy Technologies, an Energy Frontier Research Center funded by the U.S. Department of Energy, Office of Science, Office of Basic Energy Sciences under award DE-SC0001015.

Supporting information for this article is available on the WWW under http://dx.doi.org/10.1002/anie.201300446.

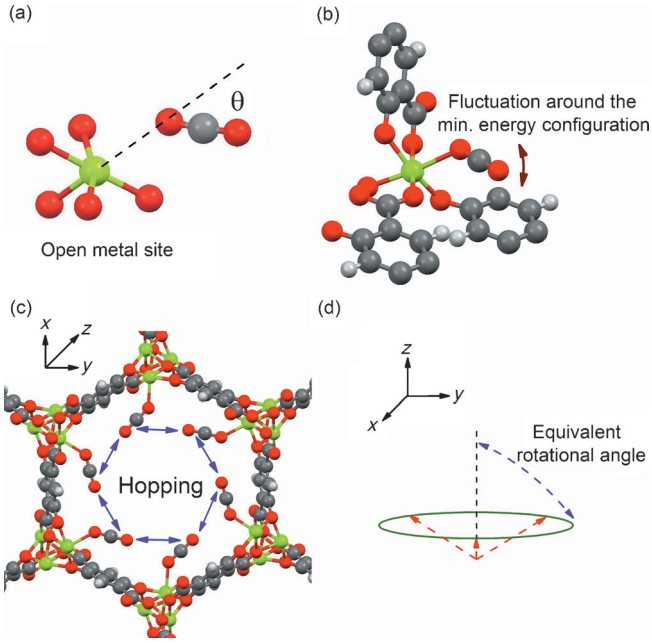

Figure 1. Schematic view of CO_2 binding in Mg-MOF-74 and its dynamics. a) Orientation of CO_2 (C gray, O red) at the minimum-energy location near a metal site (Mg green), b) localized CO_2 fluctuation motion in which the oxygen atom of the CO_2 remains bound to the same metal site, and c) nonlocalized hopping motion. The *z*-axis in the plot corresponds to the crystallographic *c*-axis. d) From an NMR point of view, the hopping of a CO_2 molecule between different metal sites in the *x*,*y* plane (see c) is equivalent to a rotation around an axis parallel to the *z*-axis with an angle referred as the "equivalent rotational angle" in this work. The CO_2 molecules (in c) in this illustration are assumed to be located at their minimum-energy configuration, and are represented by the dashed red lines.

atomic partial charges of the framework atoms were computed using the REPEAT algorithm.[13]

In carrying out the Monte Carlo simulations, we are probing equilibrium configurations. In order to make meaningful comparisons with the NMR experiments, these equilibrium configurations must be carefully interpreted in the context of CO_2 dynamics. In our simulations, we observe (see Section 4 in the Supporting Information) two types of motion: 1) fluctuation of the CO_2 molecule near the minimum-energy configuration (illustrated in Figure 1b) and 2) hops of the CO_2 molecules between different metal sites (Figure 1c). Accordingly, in our analysis we compute the CSA patterns[14] for these two different cases (see Section 1-VI in the Supporting Information for details).

At sufficiently low temperatures, we expect CO_2 to be localized near a single metal site with minimal motion. With the onset of motion, localized fluctuations and nonlocalized hops are expected to contribute differently to the motion-averaged NMR CSA pattern. Comparison of the NMR data and our simulation at $T = 100$ K shows that the simulated pattern corresponding to the localized fluctuations (Figure 2a, dashed red line) agrees with the experimental spectrum (Figure 2b), while the simulated pattern including hopping between metal sites (Figure 2a, blue lines) has a qualitatively different CSA pattern. The slight asymmetry of the CSA pattern calculated with the localized fluctuations (Figure 2a, dashed red line) reflects the asymmetry of the motion (see Figures SI 6–8 in the Supporting Information; the 2D projected plots demonstrate the asymmetric free energy surface near a metal site). This small asymmetry is not apparent in the experimental data owing to dipolar broadening from nearby linker protons.[4] At higher temperatures, the experimental patterns, which show uniaxial rotational motions, clearly deviate from the simulated patterns based on the fluctuation motions (Figure 2a, dashed red line).

To properly account for the experimental NMR data at higher temperatures, we consider hopping motions of CO_2 between different metal sites in the *x*,*y* plane (Figure 1c). It is important to realize that the NMR experiment only measures the relative orientation of the CO_2 molecule with respect to the applied magnetic field. Figure 1c shows the six minimum-energy CO_2 configurations obtained from DFT calculations.[10] If a CO_2 molecule hops between these configurations, the observed NMR signal is equivalent to a uniaxial rotation. This is best imagined by defining a common origin at the oxygen atom of the CO_2 molecule that is bound to the metal

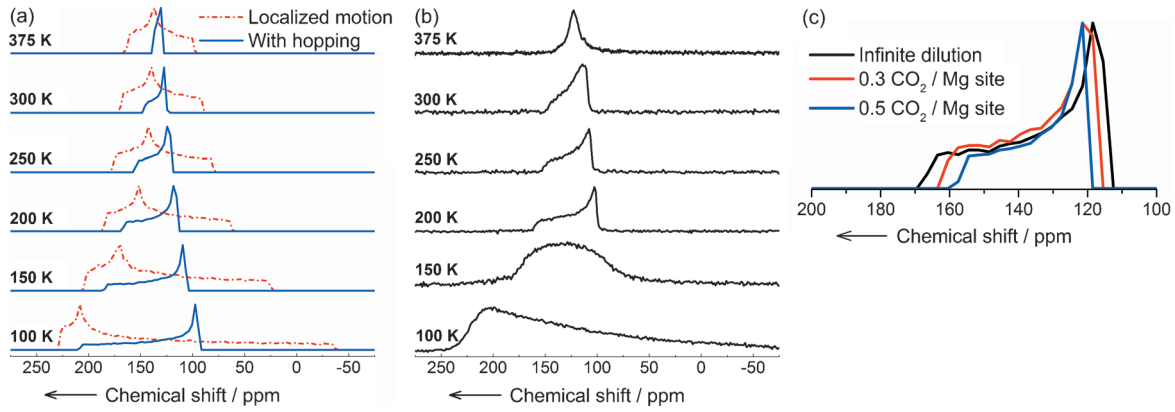

Figure 2. Comparison between simulated and experimental CSA patterns and the effect of CO_2 loading on the CSA patterns in Mg-MOF-74. a) Simulated patterns with CSA tensor values of $\sigma_\perp = 245$ ppm and $\sigma_\parallel = -90$ ppm[14] at infinite dilution for localized fluctuation motions (red dashed line) and including nonlocalized hopping motions (blue line). b) Experimental patterns at 0.5 CO_2/Mg site.[4] c) Simulated CSA patterns at 200 K with different loadings: infinite dilution (black), 0.3 CO_2/Mg site (red), and 0.5 CO_2/Mg site (blue).

site. Because of the symmetry of the crystal, these minimum-energy configurations are related through a uniaxial rotation of 80° (see Section 3 in the Supporting Information), a fixed angle, which we define as the "equivalent rotational angle" (see Figure 1 d). Hence, from an NMR point of view, hopping between these sites creates a CSA pattern that is identical to that predicted from uniaxial rotation about this equivalent angle. With the hopping motions, the simulated pattern at 100 K has an equivalent rotation angle of 71°. However, the temperature is too low here to observe hopping, which becomes possible above 200 K.

At $T > 200$ K, the experimental NMR lineshape is consistent with uniaxial rotation at an angle of approximately 60°,[4] which is the equivalent rotational angle we calculate by including hopping between sites. Moreover, our simulations show that the equivalent rotational angle decreases with increasing temperature, with values of 61° and 57° at 200 K and 300 K, respectively. The apparent decrease in the equivalent rotational angle with increasing temperature is seen as a manifestation of thermally activated motion along the z-direction (see Section 4 in the Supporting Information; the changes of the $C(CO_2)$ position along the z-direction are shown in Figures SI 7 and 8 in the Supporting Information). Enhanced motion along the z-direction results in a larger tilt angle of the CO_2 molecules with respect to the x,y plane, which is the effect that decreases the equivalent rotational angle.

The experimental CSA pattern at 150 K (Figure 2 b) reveals a transition behavior that mixes both the localized and the nonlocalized CO_2 movements. We expect that this temperature is just high enough to allow the CO_2 molecules to hop between the different metal sites, but at the same time low enough to categorize hopping as a rare event. This transition temperature is an exquisite probe of the energetics of CO_2 hopping.

Figure 2 c shows the effect of changing the CO_2 loading on the simulated CSA pattern. The results indicate that there is a shift in the pattern for larger loading values, which leads to smaller equivalent rotation angles (i.e., 60° and 59° at the loadings of 0.3 CO_2/Mg site and 0.5 CO_2/Mg site, respectively). This shift to smaller rotational angles is also what is observed experimentally. As the number of CO_2 molecules inside the structure increases, the repulsive forces between CO_2 molecules cause them to stay apart along the channel (z-direction) from each other, enlarging the angle of CO_2 adsorbed at open metal sites with respect to the x,y plane.

We can use the knowledge gained from this study to make a prediction regarding the CSA pattern of CO_2 in a similar structure: Mg_2(dobpdc) (dobpdc^{4-} = 4,4′-dioxido-3,3′-biphenyldicarboxylate), which is an expanded MOF-74 structure owing to an extended organic linker.[15] In this structure, the smallest Mg–Mg separations within a channel are 10.82 Å in the x,y plane, while the corresponding separations in Mg-MOF-74 are 8.22 Å. (see Figures SI 1 and 2 for visualizing the structures). The local dynamics of adsorbed CO_2 in the expanded MOF is expected to be similar to those for Mg-MOF-74. The difference between these two structures is that the longer ligand might make it more difficult for the CO_2 molecule to hop between metal sites. Figure 3 illustrates the

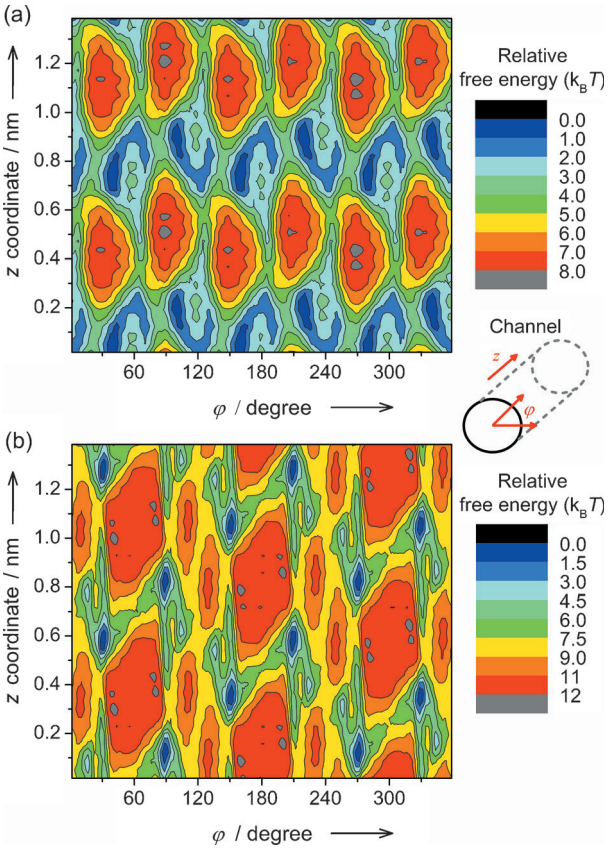

Figure 3. Free energy map of a cylinder-like channel in a) Mg-MOF-74 and in b) Mg_2(dobpdc) at 200 K is shown as a function of the angular angle φ of the channel opening and the position of the channel along the z-direction. The minimum free energy binding site near an open metal site was set to be zero $k_B T$ in this illustration.

CO_2 free energy map[16] within a cylinder-like channel for these two structures at 200 K. The angular angle of the channel opening and the position along the direction of the channel (i.e., z-direction) were utilized to map the entire channel profile. These maps show that a CO_2 molecule can hop to the two neighboring sites in the x,y plane and along the Mg-O-Mg backbone in the z-direction. It is important to note that hops along the z-direction do not change the orientation of the molecules. Although these hops are important for diffusion, they are not probed by the NMR methods reported previously.[4] The maps show that the free energy barrier for hopping between two adjacent sites along the x,y plane in the expanded structure is two times larger than what is computed for Mg-MOF-74. Given that the uniaxial rotation-like CSA pattern originates from CO_2 hops between different metal sites, the jumps should occur less frequently within the pores of the expanded structure. As a result, we predict a higher transition temperature for the expanded Mg-MOF-74 structure in which the purely localized motions become mixed with the hopping motions. Figure 4 further shows the experimental CSA pattern obtained for Mg_2(dobpdc). Comparison of NMR lineshapes between Mg-MOF-74 (Figure 2 b) and the expanded structure (Figure 4) indicates that the pattern that has the signature of the hopping motions indeed shifts to

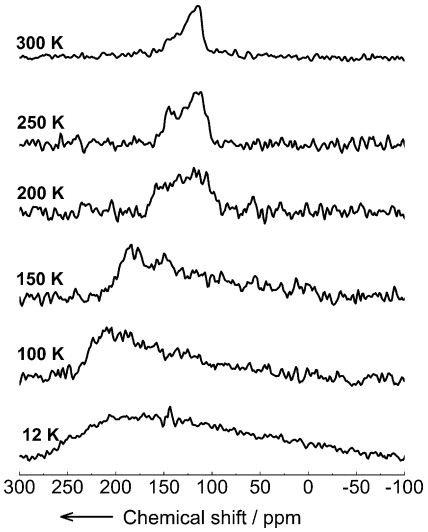

Figure 4. Experimental CSA patterns for Mg_2(dobpdc), an expanded variant of Mg-MOF-74, at a loading of 0.4 CO_2/Mg site and at various temperatures from 12 K to 300 K.

higher temperatures, $T = 150$–200 K in Mg-MOF-74 and $T \approx 250$ K in Mg_2(dobpdc). It would be interesting to investigate how this change in the dynamics depends on the length of the linkers.[17]

In summary, we have proposed a dynamic mechanism that provides an alternative explanation for the experimental CSA pattern than the one put forward previously.[4] We argue that the more proper interpretation of the NMR signal is not a uniaxial rotation at the open metal site, but a signature of the hopping motions between different metal sites. We re-emphasize that obtaining detailed information regarding the CO_2 dynamics is important and this work illustrates that the dynamics is much richer than initially expected.

Received: January 18, 2013
Published online: March 28, 2013

Keywords: carbon dioxide capture · chemical shift anisotropy · CO_2 dynamics · metal–organic frameworks

[1] a) D. M. D'Alessandro, B. Smit, J. R. Long, *Angew. Chem.* **2010**, *122*, 6194 – 6219; *Angew. Chem. Int. Ed.* **2010**, *49*, 6058 – 6082; b) L.-C. Lin, A. H. Berger, R. L. Martin, J. Kim, J. A. Swisher, K. Jariwala, C. H. Rycroft, A. S. Bhown, M. W. Deem, M. Haranczyk, B. Smit, *Nat. Mater.* **2012**, *11*, 633 – 641; c) K. Sumida, D. L. Rogow, J. A. Mason, T. M. McDonald, E. D. Bloch, Z. R. Herm, T.-H. Bae, J. R. Long, *Chem. Rev.* **2012**, *112*, 724 – 781.

[2] M. Dincă, J. R. Long, *Angew. Chem.* **2008**, *120*, 6870 – 6884; *Angew. Chem. Int. Ed.* **2008**, *47*, 6766 – 6779.

[3] a) N. L. Rosi, J. Kim, M. Eddaoudi, B. Chen, M. O'Keeffe, O. M. Yaghi, *J. Am. Chem. Soc.* **2005**, *127*, 1504 – 1518; b) S. R. Caskey, A. G. Wong-Foy, A. J. Matzger, *J. Am. Chem. Soc.* **2008**, *130*, 10870 – 10871; c) D. Britt, H. Furukawa, B. Wang, T. G. Glover, O. M. Yaghi, *Proc. Natl. Acad. Sci. USA* **2009**, *106*, 20637 – 20640; d) P. D. C. Dietzel, V. Besikiotis, R. Blom, *J. Mater. Chem.* **2009**, *19*, 7362 – 7370; e) J. M. Simmons, H. Wu, W. Zhou, T. Yildirim, *Energy Environ. Sci.* **2011**, *4*, 2177 – 2185; f) J. A. Mason, K. Sumida, Z. R. Herm, R. Krishna, J. R. Long, *Energy Environ. Sci.* **2011**, *4*, 3030 – 3040; g) E. D. Bloch, L. J. Murray, W. L. Queen, S. Chavan, S. N. Maximoff, J. P. Bigi, R. Krishna, V. K. Peterson, F. Grandjean, G. J. Smit, B. Smit, S. Bordiga, C. M. Brown, J. R. Long, *J. Am. Chem. Soc.* **2011**, *133*, 14814 – 14822.

[4] X. Kong, E. Scott, W. Ding, J. A. Mason, J. R. Long, J. A. Reimer, *J. Am. Chem. Soc.* **2012**, *134*, 14341 – 14344.

[5] R. Krishna, J. M. van Baten, *J. Phys. Chem. C* **2012**, *116*, 23556 – 23568.

[6] a) L. Valenzano, B. Civalleri, S. Chavan, G. T. Palomino, C. Arean, S. Bordiga, *J. Phys. Chem. C* **2010**, *114*, 11185 – 11191; b) R. Poloni, B. Smit, J. B. Neaton, *J. Phys. Chem. A* **2012**, *116*, 4957 – 4964; c) Y. Yao, N. Nijem, J. Li, Y. J. Chabal, D. C. Langreth, T. Thonhauser, *Phys. Rev. B* **2012**, *85*, 064302.

[7] W. L. Queen, C. M. Brown, D. K. Britt, P. Zajdel, M. R. Hudson, O. M. Yaghi, *J. Phys. Chem. C* **2011**, *115*, 24915 – 24919.

[8] D. Frenkel, B. Smit, *Understanding Molecular Simulations: from Algorithms to Applications*, 2nd ed. Academic Press, San Diego, **2002**.

[9] J. Kim, R. L. Martin, O. Rübel, M. Haranczyk, B. Smit, *J. Chem. Theory Comput.* **2012**, *8*, 1684 – 1693.

[10] A. L. Dzubak, L.-C. Lin, J. Kim, J. A. Swisher, R. Poloni, S. N. Maximoff, B. Smit, L. Gagliardi, *Nat. Chem.* **2012**, *4*, 810 – 816.

[11] A. K. Rappe, C. J. Casewit, K. S. Colwell, W. A. Goddard, W. M. Skiff, *J. Am. Chem. Soc.* **1992**, *114*, 10024 – 10039.

[12] J. J. Potoff, J. I. Siepmann, *AIChE J.* **2001**, *47*, 1676 – 1682.

[13] C. Campañá, B. Mussard, T. K. Woo, *J. Chem. Theory Comput.* **2009**, *5*, 2866 – 2878.

[14] A. J. Beeler, A. M. Orendt, D. M. Grant, P. W. Cutts, J. Michl, K. W. Zilm, J. W. Downing, J. C. Facelli, M. S. Schindler, W. Kutzelnigg, *J. Am. Chem. Soc.* **1984**, *106*, 7672 – 7676.

[15] T. M. McDonald, W. R. Lee, J. A. Mason, B. M. Wiers, C. S. Hong, J. R. Long, *J. Am. Chem. Soc.* **2012**, *134*, 7056 – 7065.

[16] B. Smit, T. L. M. Maesen, *Chem. Rev.* **2008**, *108*, 4125 – 4184.

[17] H. Deng, S. Grunder, K. E. Cordova, C. Valente, H. Furukawa, M. Hmadeh, F. Gándara, A. C. Whalley, Z. Liu, S. Asahina, H. Kazumori, M. O'Keeffe, O. Terasaki, J. F. Stoddart, O. M. Yaghi, *Science* **2012**, *336*, 1018 – 1023.

